

The origin of massive nonlinearity in Mixed-Ionic-Electronic-Conduction (MIEC)–based Access Devices, as revealed by numerical device simulation

A. Padilla, G. W. Burr, R. S. Shenoy, K. V. Raman[§], D. Bethune, R. M. Shelby, C. T. Rettner, J. Mohammad, K. Virwani, P. Narayanan, A. K. Deb[§], R. K. Pandey[†], M. Bajaj[†], K. V. R. M. Murali[†], B. N. Kurdi and K. Gopalakrishnan[‡]
IBM Research – Almaden, 650 Harry Road, San Jose, CA 95120 ([‡]IBM T. J. Watson Research Center, Yorktown Heights, NY 10598)
([§]IBM India Research Labs, Bangalore KA, India 560045) ([†]IBM SRDC India, Bangalore KA, India 560045)
Tel: (408) 927–1512, Fax: (408) 927–2100, E-mail: gwburr@us.ibm.com

Abstract

Numerical modeling is used to explain the origin of the large ON/OFF ratios, ultra-low leakage, and high ON current densities exhibited by BEOL-friendly Access Devices (AD) based on Cu-containing MIEC materials [1-5]. Motion of large populations of copper ions and vacancies leads to exponential increases in hole current, with a turn-ON voltage that depends on material bandgap. Device simulations match experimental observations as a function of temperature, electrode aspect-ratio, thickness, and device CD.

Keywords: Access device, MIEC, NVM, PCM, RRAM, MRAM

Introduction

Mixed-Ionic-Electronic-Conduction (MIEC)-based ADs [1–5] exhibit ideal characteristics for 3D-stacking of large crosspoint arrays of any resistive nonvolatile memory (NVM) in the BEOL, including bipolar diode-like characteristics (Fig. 1), large ON/OFF ratios, high voltage margin V_m (for which leakage stays below 10 nA), ultra-low leakage (< 10 pA), and high ON current densities. Although dependent on total electrode area [1,2,4], the V_m of any given MIEC device structure is mostly independent of the size of the gap between the two electrodes, d_{gap} (Fig. 2). In addition, transient response is markedly faster for points higher up the I–V curve (Fig. 3), with turn-on times varying from $> 1\mu\text{sec}$ (for $I \ll 1\mu\text{A}$) to 15nsec for $I > 100\mu\text{A}$ [4].

The operation of MIEC devices has been qualitatively attributed to the modulation of electronic current by the motion of Cu ions [1,5]. In this work, we quantify this theory using Sentaurus TCAD. Adapting features for tracking mobile H^+ ions [6], we perform 2–D numerical device simulations of Cu-based MIEC semiconductors containing large concentrations of mobile positive Cu^+ ions and negative V_{Cu}^- vacancies. Cu^+ ions are allowed to interact with conduction electrons, yet V_{Cu}^- vacancies do not interact with holes. The simulator self-consistently solves the continuity and Poisson equations, along with ionization-recombination kinetics (Fig. 4) and a ‘Unified Contact’ Schottky model [7] at each ion-blocking metal electrode. While 1–D models have been developed (Fig. 5), none have incorporated Schottky interfaces, minority carriers, and electron-ion recombination simultaneously.

Modeling MIEC ADs

In the absence of ions, a metal-semiconductor-metal (MSM) structure is simply two Schottky diodes connected back-to-back. As bias increases, current originally limited by the reverse-biased diode increases due to minority-carrier diffusion. However, unlike MIEC ADs, turn-on voltages V_m are large and depend strongly on d_{gap} (Fig. 6).

In such a p-type MSM structure, a metal work-function very close to the valence band should imply large current flow even at low bias voltages. The large number of mobile positive ions in Cu-containing MIEC materials (Fig. 7) interact with conduction-band electrons and change this behavior markedly (Fig. 8). At zero bias (Fig. 9(a)), mobile ions settle into a U-shaped distribution with large electric fields at each interface, maintaining a dynamic equilibrium between electrostatic ion drift towards, and ion diffusion away from, each interface [8]. This ion accumulation results in narrow depletion widths and residual electron tunneling at each interface, yet strong suppression of holes and hole current.

At low bias, holes are injected from the positively-biased electrode (Fig. 9(b)), eventually resulting in significant hole diffusion

current (with a characteristic SS of ~ 85 mV/dec) as the device transitions out of the OFF-state dominated by electron current. Copper ions move away from (and vacancies move towards) the positive electrode, where current is limited at high bias by hole tunneling. Hall-effect measurements performed on MIEC-based materials (Fig. 8, inset) confirm hole-dominated currents at large carrier densities. This behavior is consistent with a suppressed interaction between V_{Cu}^- vacancies and holes (large energy barrier), unlike the interaction between Cu^+ ions and electrons.

Role of Electrode Gap

Within a device with a large electrode-gap d_{gap} , a distinct ‘quasi-neutral’ region where $[\text{Cu}^+] \sim [\text{V}_{\text{Cu}}^-]$ separates the regions of extreme ion aggregation at each interface. This allows the device characteristics to be independent of d_{gap} until these interfacial regions begin to interfere with each other, leading to a decrease in the voltage margin V_m (at 10nA) (Fig. 10). Filaments are not modeled here, but may also form across a narrow d_{gap} . While simulated trends of V_m do show an increase as devices are scaled in CD (Fig. 10), the trend is not as strong as that seen experimentally [2].

Device Asymmetry and Transient Response

Simulated IV characteristics become asymmetric for devices with highly asymmetric electrode areas, such as conductive-AFM measurements of blanket films (Fig. 11), and show an increase in leakage current as temperature increases. Transient simulations of the MIEC AD response (Fig. 12) show rapid response at high bias and high current, with a slower response at low bias and low current, similar to experiments (Fig. 3). However, the modeled interplay — between fast ion migration that turns on the device, and the slower interaction between ions and electrons that allows hole current to dominate (Fig. 13) — does not exhibit the same vast dynamic range in response speeds (from $\sim 25\text{ns}$ to $\sim 100\text{ms}$) observed experimentally, suggesting that further model refinement, possibly involving interfacial Cu^+ reduction, will be necessary. Finally, by carefully tuning simulation mesh against TEM images, precise matching of IV characteristics can be obtained (Fig. 14).

Conclusions

A commercial device simulator was adapted to explain the large ON/OFF ratios, ultra-low leakage, and high ON current densities offered by BEOL-friendly Access Devices (AD) based on Cu-containing Mixed-Ionic-Electronic-Conduction (MIEC) materials [1-5]. Ultra-low leakage at low bias is due to residual electron tunneling, with hole current suppressed by a central ‘quasi-neutral’ region. Device turn-on occurs as hole injection from the positively-biased electrode increases sharply, driven by motion of large populations of copper ions and vacancies. Simulated trends in turn-on voltage V_m vs. d_{gap} and CD, transient response, temperature dependence, and highly asymmetric device geometries all match experimental observations.

References

- [1] K. Gopalakrishnan et. al., *VLSI Tech. Symp.*, 19.4 (2010).
- [2] R. S. Shenoy et. al., *VLSI Tech. Symp.*, 5B.1 (2011).
- [3] G. W. Burr et. al., *VLSI Tech. Symp.*, T5.4 (2012).
- [4] K. Virwani et. al., *IEDM Tech. Digest*, 2.7 (2012).
- [5] G. W. Burr et. al., *VLSI Tech. Symp.*, T6.4 (2013).
- [6] Sentaurus TCAD, www.synopsys.com (2012).
- [7] M. Jeong et. al., *IEDM Tech. Digest*, 733 (1998).
- [8] J. Maier, in *Prog. Solid St. Chem.* **23** 171 (1995).

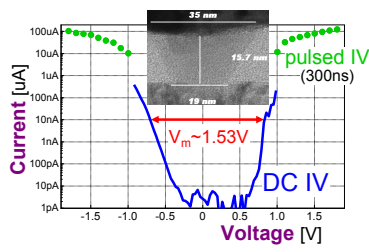


Fig. 1 Access Devices (ADs) based on Cu-containing Mixed-Ionic-Electronic-Conduction (MIEC) materials exhibit bipolar diode-like characteristics with ultra-low leakage and large ON/OFF ratios [1-5].

| Reference: | Models: | Ignores: | Results: |
|--|--|--|---|
| Arlibart et al. <i>Electrochimica Acta</i> 24 (1978) | <ul style="list-style-type: none"> p-type semiconductor mobile Cu⁺ & holes Fixed acceptors Cu⁺ reduction at cathode | <ul style="list-style-type: none"> minority carriers Schottky/ohmic nature of contacts | 1D Model predicts linear dc IV curves |
| Gil et al. <i>Solid State Ionics</i> 179 (2008) | <ul style="list-style-type: none"> MSM structure mobile acceptors & holes OR mobile donors & electrons | <ul style="list-style-type: none"> minority carriers Schottky/ohmic nature of contacts | 1D Model predicts various dc IV curves |
| Strukov et al. <i>Small</i> 5, No. 9 (2009) | <ul style="list-style-type: none"> MSM structure mobile ions, electrons, holes Fixed acceptors bulk-limited transport, with ohmic contacts for electrons | <ul style="list-style-type: none"> electron-ion recombination kinetics Schottky nature of contacts | 1D Model predicts recombination IV curves |

Fig. 5 1D Metal-MIEC-Metal models proposed previously — none combine Schottky interfaces, minority carriers, and electron-ion recombination.

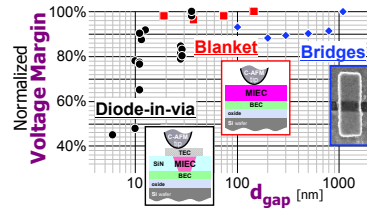


Fig. 2 Measured turn-on voltages depend strongly on device CD [2] (not shown), but are insensitive to the gap between electrodes (d_{gap}) down to very small thicknesses.

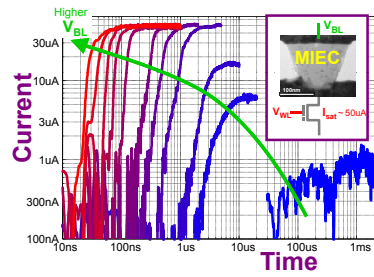


Fig. 3 Larger applied voltages with higher saturation currents lead to faster turn-on of MIEC access devices.

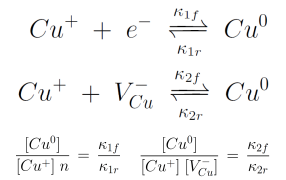


Fig. 4 Sentaurus TCAD [6] is used to model drift, diffusion, and two rate-equation interactions between mobile copper ions (Cu^+), atoms (Cu^0), mobile vacancies (V_{Cu}^-), and electrons.

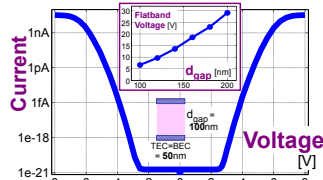


Fig. 6 While a simulated MSM structure without ions has an MIEC-like IV, currents are too low and ON-transition voltages are large and depend strongly on d_{gap} .

$$E_g = 1.4 \text{ eV} \quad D_{Cu^+} = D_{V_{Cu}^-} = 8e-4 \text{ cm}^2/\text{s}$$

$$\phi_M = 5.375 \text{ eV} \quad [Cu^0] = 1e21 \text{ cm}^{-3}$$

$$\chi = 4.05 \text{ eV}$$

$$\kappa_{1f}, \kappa_{1r} = 3e-9, 6e2 \text{ cm}^{-3} \text{ s}^{-1}$$

$$\kappa_{2f}, \kappa_{2r} = 1.86e-9 e^{-0.1955/k_B T}, 1e3 \text{ cm}^{-3} \text{ s}^{-1}$$

Fig. 7 Important parameters in our numerical model for MIEC ADs include bandgap E_g , the large number of copper atoms (Cu^0) contributing mobile ions (Cu^+) and vacancies (V_{Cu}^-), and the associated interaction rates (Fig. 4).

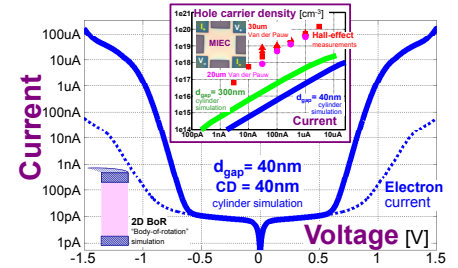


Fig. 8 Simulated IV curve for a cylindrical MIEC AD. As bias increases, electron-dominated current gives way to holes, matching Hall-effect measurements (inset).

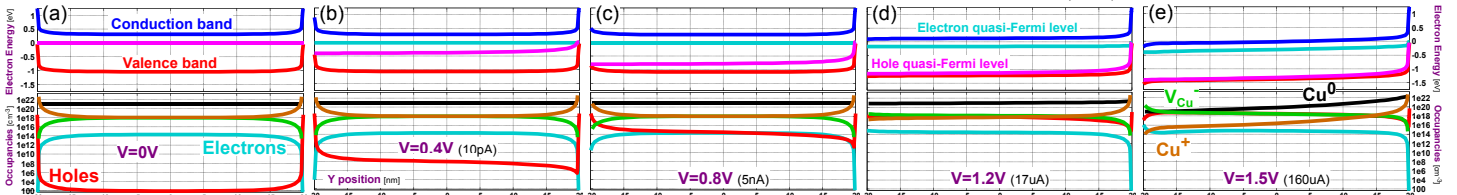


Fig. 9 At zero bias (a), the large number of mobile positive ions settle into a U-shaped distribution with large electric fields at each interface, maintaining dynamic equilibrium between electrostatic ion drift towards, and ion diffusion away from, each interface. This ion accumulation results in narrow depletion widths and residual electron tunneling at each interface, yet strong suppression of holes and hole current. As bias increases (b,c,d), holes are injected from the positively-biased electrode (TEC, at left), the hole barrier presented by the valence band shrinks, and hole current increases exponentially. Copper ions move away from (and vacancies move towards) the TEC, where current is limited at high bias by hole tunneling. At high bias (e), Cu^0 , the lattice copper sites that can contribute ions, are depleted at the TEC side and over-saturated at the BEC side, possibly initiating damage of the material.

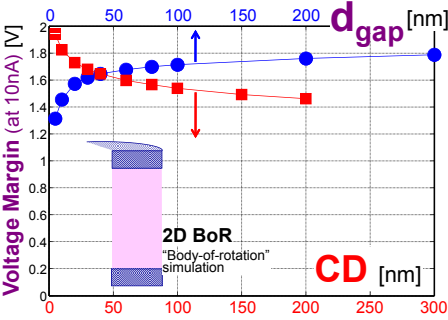


Fig. 10 Variation in simulated voltage margin as thickness (d_{gap}) and diameter (CD) vary around the CD = 40nm, d_{gap} = 40nm cylinder shown in Fig. 8.

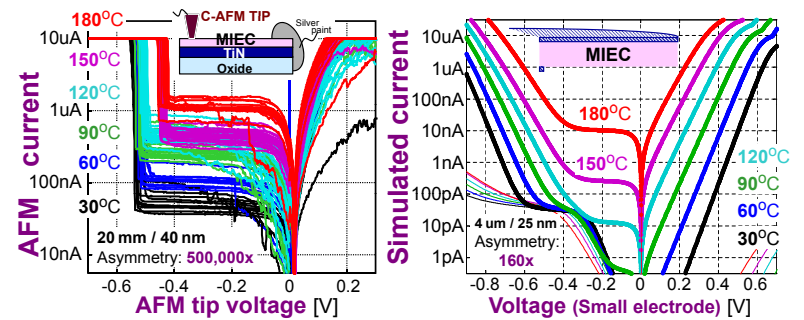


Fig. 11 (a) Conductive-AFM measurements of blanket films show highly asymmetric IV characteristics because of the large asymmetry in electrode areas, and noise floor increases with temperature. These features can be (b) qualitatively matched in simulation.

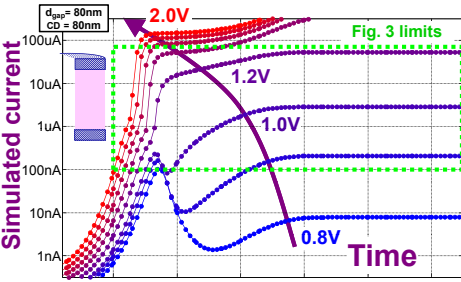


Fig. 12 Transient simulations of MIEC AD response show that the ion migration needed to turn on an MIEC AD occurs slowly at low bias and current, yet rapidly at high bias and current, although not with the same wide dynamic range observed in experiments (Fig. 3). Transient data at higher temperature is likely to be faster, accommodated by adjusting the rate constants in Figs. 4 & 7 with the appropriate energy barriers.

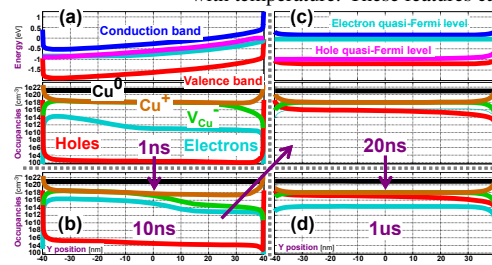


Fig. 13 After a voltage ramp to 1.0V (a, 1ns), hole occupancy remains suppressed by the large Cu^+ population diffusing slowly away from the positive (left) interface (b, 10ns). After 20ns (c), this ion population has departed, flattening the bands and allowing some hole injection. By 1us (d), the slow interaction between Cu^+ and electrons has suppressed electron current, allowing hole current to dominate.

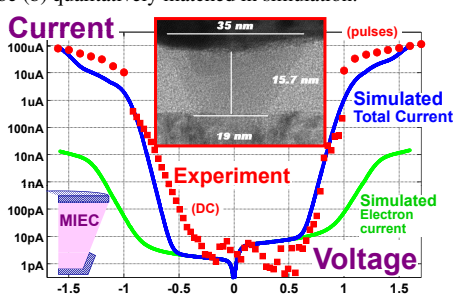


Fig. 14 By carefully tuning the simulation mesh against TEM images for dimensions and the slight recess into the bottom electrode, precise matching of IV characteristics can be obtained, including ultra-low leakage currents, voltage turn-ON values, and >7 orders of magnitude in ON-OFF ratio.